J. of the Environmental Sciences
Vol. 13, No. 8, 721~731, 2004

Recycling of Suspended Particulates by Atmospheric Boundary Depth and Coastal Circulation

Hyo Choi

Dept. of Atmospheric Environmental Sciences, Kangnung National University, Gangneung, 210-702, Korea

(Manuscript received 8 November, 2003 ; accepted 1 June, 2004)

The dispersion of suspended particulates in the coastal complex terrain of mountain- inland basin (city)-sea, considering their recycling was investigated using three-dimensional non-hydrostatic numerical model and lagrangian particle model (or random walk model). Convective boundary layer under synoptic scale westerly wind is developed with a thickness of about 1 km over the ground in the west of the mountain, while a thickness of thermal internal boundary layer (TIBL) is only confined to less than 200m along the eastern slope of the mountain, below an easterly sea breeze circulation. At the mid of the eastern slop of the mountain, westerly wind confronts easterly sea breeze, which goes to the height of 1700 m above sea level and is finally eastward return flow toward the sea. At this time, particulates floated from the ground surface of the city to the top of TIBL go along the eastern slope of the mountain in the passage of sea breeze, being away the TIBL and reach near the top of the mountain. Then those particulates disperse eastward below the height of sea-breeze circulation and widely spread out over the coastal sea. Total suspended particulate concentration near the ground surface of the city is very low. On the other hand, nighttime radiative cooling produces a shallow nocturnal surface inversion layer (NSIL) of 200 m thickness over the inland surface, but relatively thin thickness less than 100m is found near the mountain surface. As synoptic scale westerly wind should be intensified under the association of mountain wind along the eastern slope of mountain to inland plain and further combine with land-breeze from inland plain toward sea, resulting in strong wind as internal gravity waves with a hydraulic jump motion bounding up to about 1km upper level in the atmosphere in the west of the city and becoming a eastward return flow. Simultaneously, wind near the eastern coastal side of the city was moderate. Since the downward strong wind penetrated into the city, the particulate matters floated near the top of the mountain in the day also moved down along the eastern slope of the mountain, reaching the downtown and merging in the ground surface inside the NSIL with a maximum ground level concentration of total suspended particulates (TSP) at 0300 LST. Some of them were bounded up from the ground surface to the 1 km upper level and the others were forward to the coastal sea surface, showing their dispersions from the coastal NSIL toward the propagation area of internal gravity waves. On the next day at 0600 LST and 0900 LST, the dispersed particulates into the coastal sea could return to the coastal inland area under the influence of sea breeze and the recycled particulates combine with emitted ones from the ground surface, resulting in relatively high TSP concentration. Later, they float again up to the thermal internal boundary layer, following sea breeze circulation.

Key Words : Suspended particulates, Lagrangian, Convective boundary layer, Thermal internal boundary layer, Sea-breeze, Land-breeze, Nocturnal surface inversion layer, Internal gravity waves, Hydraulic jump motion

1. Introduction

During the past decade empirical and numerical studies have been carried out the prediction on pollutant concentrations over coastal complex terrain, but their accuracies on the dispersion and diffusion of particulate matters have been in still uncertainties, due to complicated wind patterns caused by topography and ocean[1~3]. Suspended particulates are not only harmful to human's health but also of great importance in heat budget in the coastal atmospheric

Corresponding Author : Hyo Choi, Dept. of Atmospheric Environmental Sciences, Kangnung National University, Gangneung 210-702, Korea
Phone : +82-33-652-0356
E-mail : choihyo@kangnung.ac.kr

boundary. High density of suspended particulates floating near the top of convective boundary layer reduces the solar energy reaching the ground surface and the reduction of solar radiation, such as dome effect.

Kuwagata and Sumioka[4] explained that local circulation system was very complicated by complex terrain and sea under the different weather condition, and Ross et al.[5] indicated that the local airshed surrounding the Comalco smelter was strongly influenced by the proximity of the ocean and the complex terrain on the Tama Valley. The increase of pollution concentration occurred under daytime photochemical reaction process in the city[6] and pollutant gases could be changed into aerosol phase through their chemical reaction process and cause the increase of local and regional air pollution concentrations[7]. Park and Moon[8] explained particle dispersion in the complex coastal terrain of Korea using lagrangian particle mode and Xuan[9] insisted high density of suspended particulates interrupt daytime convection process of air near the ground surface, resulting in the decrease of vertical mixing depth of air in the boundary layer and then sequentially increasing total suspended particulate concentrations.

Since to compute the dust emission factors of the city is very hard due to the problem of lack of necessary input data such as emission rate, chemical processes among different species, meteorological impact to the transportation and diffusion of particulates[10], this study was mainly confined to investigate how total suspended particulate concentration could vary under the influence of their recycling in the coastal complex terrain using both three dimensional meteorological model and random walk model.

2. Numerical analysis and data

A three-dimensional non-hydrostatic grid point model in a complex terrain-tendency coordinate (x, y, z*), called LASV-5 model was adopted for a 48 hour numerical simulation on meteorological phenomena from 0900LST, August 13 to 0900 LST, August 15, 1995, using Hitachi super computer at Japan Meteorological Research Institute (JMRI)[11]. Two different domains consist of 50×50 grid points with a uniform horizontal interval as 20km in a coarse-mesh model and 5km in a fine-mesh for one-way double nesting, respectively. Sixteen levels in the vertical coordinate were divided from 10m into 6km with a sequentially large interval such as 10m, 40m, --, 6km, respectively. Twelve hourly global analysis data of wind, potential temperature, specific humidity, atmospheric pressure made by Japan Meteorological Agency (JMA), horizontally and vertically interpolated for two coarse and fine mesh models with different resolutions. Initial data of sea surface temperature for the model were provided by satellite picture[12].

2.1. Meteorological model

The model called LASV-5 is originally devised by JMRI, JMA and consists of a three-dimensional hydrostatic and non-hydrostatic models with a terrain-tendency coordinate system (x, y, z^*) based upon Boussinesq and anelastic approximations[13,14]. The equations of motion, where z^* is the terrain-following vertical coordinate was defined as θ, $\bar{\theta}$, T, P_{00}, π_m, π, π', z, z_T, z_G and K_m imply potential temperature (K), mean potential temperature of the model domain, air temperature at a given height, atmospheric pressure at reference (=1000 mb), Exner function of the model atmosphere, Exner function of isentropic atmosphere ($\theta=\bar{\theta}$), deviation of π, height of upper boundary with its change for time and place in a model domain, height of topography and vertical diffusion coefficient for turbulent momentum (m^2s^{-1}), respectively. f, g, u, v, w and w^*, P, P_{00}, R_d and C_p are Coriolis parameter, gravity (ms^{-2}), velocity components in the x, y, z and in the z^* coordinate, atmospheric pressure, atmospheric pressure at reference level, gas constant for dry air and specific heat at constant pressure.

Radiative heating of air was evaluated from thermodynamic equation and conservation of water vapor on potential temperature and specific humidity of water vapor. Assuming that horizontal scale of the phenomena is one order greater than vertical scale, the equation for hydrostatic equilibrium case can be converted into hydrostatic pressure deviation with a non-hydrostatic calculation and in the similar way, non-hydrostatic pressure equation is given with a non-hydrostatic calculation. For the time integration and the vertical direction in the z^* coordinate were calculated by adopting Euler-backward scheme and Crank-Nicholson scheme. The atmospheric pressure changes at the top of model atmosphere with a material surface were controlled by wave radiation condition suggested by Klemp and Durran[15], in order

to avoid reflections of gravity waves generated in the lower layers. Periodic lateral boundary condition developed by Orlanski[16] was applied to the calculation of u, v, θ and q in this model domain. In our numerical simulation, time interval, $\triangle t$=30 sec in the coarse-mesh model and $\triangle t$=10 sec in the fine- mesh are determined to effectively reduce external gravity waves appeared in the equations, especially for the non-hydrostatic model.

The vertical diffusion coefficients, K_m and K_h for momentum and heat in the surface boundary layer were evaluated from the turbulent closure level-2 model[17,18]. For evaluating total net flux of long wave radiation absorbed by water vapor and carbon dioxide and flux from the ground surface toward the upper levels, H_2O and CO_2 transmission functions, effective vapor amount, specific humidity (gcm^{-2}), pressure (mb) at the surface and arbitrary levels were considered. Total net solar radiation at the ground with a function of solar zenith angle, latitude, declination and time angle is calculated by Katayama[19]'s simplified scheme for computing radiative transfer in the troposphere.

Newtonian cooling due to long wave radiation and radiative heating rate for air and soil temperatures near the surface were consider in detail. For energy budget near the surface, the surface boundary layer was assumed to be a constant flux layer for estimating sensible and latent heat fluxes and the similarity theory is adopted[20,21]. On the time variation of soil temperature and specific humidity at the ground surface, a force restore method suggested by Deardorff[22] was employed.

2.2. Random walk model

Random walk model[11] can be given by

$$\begin{aligned} \triangle x &= u\triangle t \\ \triangle y &= v\triangle t \\ \triangle z &= w\triangle t \end{aligned} \tag{1}$$

and advection term is carried out by (ξ, η, ζ) coordinate as

$$\begin{aligned} u^* &= \frac{\partial \xi}{\partial x}u + \frac{\partial \eta}{\partial x}v + \frac{\partial \zeta}{\partial x}w \\ v^* &= \frac{\partial \xi}{\partial y}u + \frac{\partial \eta}{\partial y}v + \frac{\partial \zeta}{\partial y}w \\ w^* &= \frac{\partial \xi}{\partial z}u + \frac{\partial \eta}{\partial z}v + \frac{\partial \zeta}{\partial z}w \end{aligned} \tag{2}$$

For the conservation of mass during the advection of particulate matters, the transformation of three dimensional wind fields calculated from z^* coordinate system of LASV-5 model into $z+(= z-z_G)$ coordinate of random walk model is necessary.

$$\begin{aligned} w^* &= \frac{z^*-h}{h-z_G}\left(\frac{\partial z_G u}{\partial x} + \frac{\partial z_G v}{\partial y}\right) + \frac{h}{h-z_G}w \\ w^+ &= -\frac{\partial z_G u}{\partial x} - \frac{\partial z_G v}{\partial y} + w \end{aligned} \tag{3}$$

The increase of dispersion distribution by diffusion processes of particles with the occurrence probability of each particle as Fickian diffusion is given by

$$d\sigma^2/dt = 2k \tag{4}$$

and occurrence probability of particle in uniform random numbers with the same dispersion has

$$\triangle x = (24k\triangle t)^{1/2}\cdot RND \tag{5}$$

where $\triangle x$ and $\triangle z$ are in the similar to $\triangle x$ and RND is uniform number of (0.5, + 0.5). If particle undergoes random walk with a small $\triangle t$, particle distribution can be as Gaussian distribution. In z^* coordinate,

$$\triangle z^* = (24k\triangle t)^{1/2}\frac{h}{h-z_G}\cdot RND \tag{6}$$

For the treatment of deposition process below the reference level ($z = \triangle z$), deposition probability of particle on the ground level can be given as

$$\begin{aligned} P &= \frac{\triangle M}{M} \\ &= \frac{v_d\triangle t}{\triangle z} \end{aligned} \tag{7}$$

where v_d is deposition velocity of particle. In no deposition of particle, a reflection condition is given. A fine-mesh domain in the particle model consists of 50×50 grid points with a uniform horizontal interval of 5km as the same as in the meteorological model. Particles in the model were emitted from the surface level of Kangnung city at the rate of four particles per two minutes. After sunset, the number of released particles was reduced like two particles per two minutes, due to the reduced number of vehicles on the street. Numerically calculated results on suspended particulate concentration were compared with measured TSP concentrations at Kangnung Environmental Observatory[24].

3. Results and Discussion

3.1. Dispersion of suspended particulate (day)

At 1200 LST, as prevailing synoptic-scale westerly wind blows over Mt. Taegullyung toward the coastal sea and easterly sea-breeze associated with upslope wind (valley wind) also comes from the sea up to the top of the mountain, two different kinds of wind regimes confront each other along the eastern slope of the mountain and then onshore wind goes up to 1400 m height, being finally a return flow toward the East Sea (Figs. 1 and 2). Convective boundary layer (CBL) is developed with a thickness of about 1km over the ground in the upwind side of the mountain, while the thickness of thermal internal boundary layer (TIBL), due to the differences of surface roughness and thermal heating at the interface of land and sea is only confined to less than 100m along the eastern slope of the mountain below an easterly sea-breeze circulation. At 1500 LST, atmospheric circulation and thermal and convective boundary layers have similar patterns as ones at 1200 LST.

At this time, suspended particulate matters also are floated by thermal convection of air from the ground surface of Kangnung city, being away from the TIBL and are uplifted by sea-breeze toward the top of the mountain. As daytime goes on, the floated particulates up to the 1400 m height are dispersed eastward below the height of sea-breeze circulation and then, widely spread out over the coastal sea surface (Fig. 3a). At 1500 LST, the floating particulates are further dispersed over the coastal sea (Fig. 3b).

3.2. Dispersion of suspended particulate (sunset and night)

Near sunset, at 1800 LST, the thickness of the TIBL due to the decrease of solar radiation become shallower and sea-breeze regime become smaller than daytime one at 1200 LST. The floating heights of particulates are much lower than those at 1500 LST and TSP concentration inside the shrunken TIBL near Kangnung city became higher. Shortly after sunset, 2100 LST, as internal gravity waves begin to be developed along the eastern slope of the mountain, relatively strong downslope wind (katabatic or mountain wind) blows toward the city, but sea-breeze circulation still exists in the offshore side (Fig. 4). Thus, the particulates move down along the eastern slope of the mountain toward the coast and the concentration of particulates at the city becomes higher

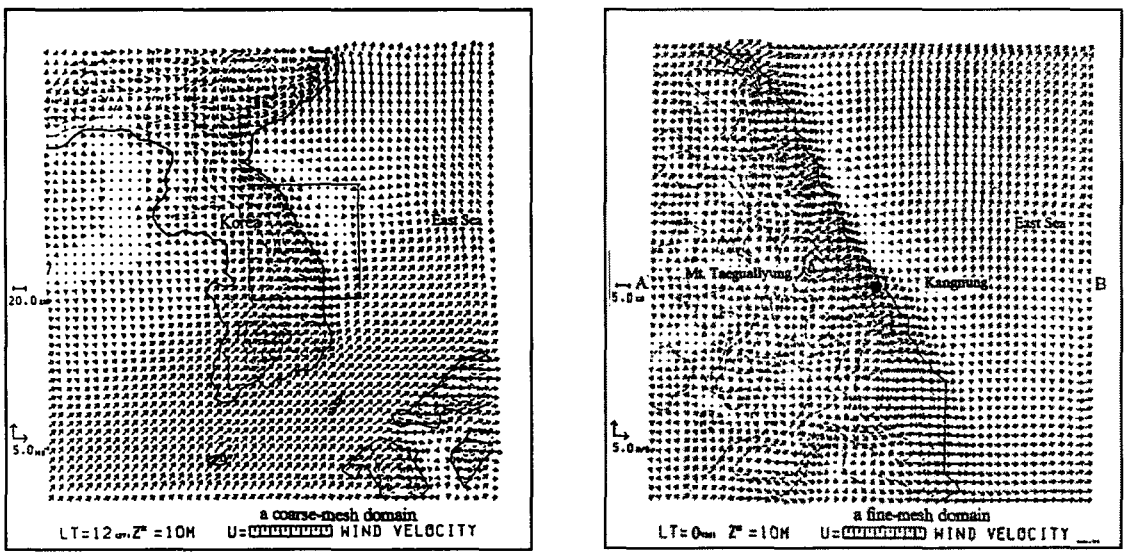

(a) (b)

Fig. 1. (a) Wind fields (ms^{-1}) in a coarse-mesh domain adjacent to Korean peninsula at 1200 LST, August 14. Thin dash line and circle o denote topography and Kangnung city. (b) A box indicates a fine-mesh domain adjacent Kangnung city with 50×50 grids of 5km each interval.

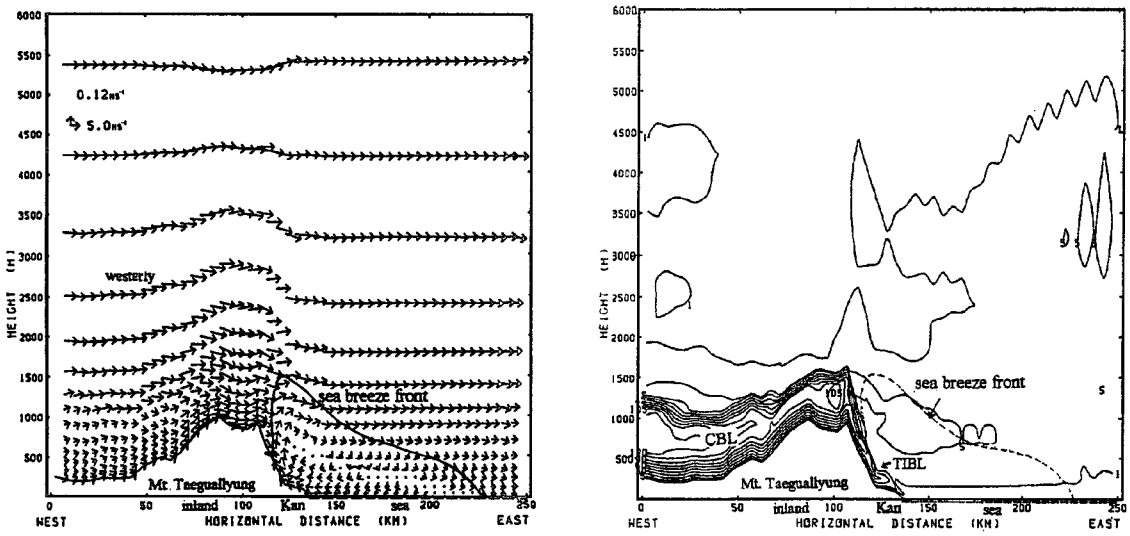

(a) (b)

Fig. 2. (a) Vertical profiles of wind (ms^{-1}) on a straight cutting line A-B (Mt. Taeguallyung-Kangnung city-East Sea) in a fine mesh domain of Fig. 1b at 1200 LST. Dash line and Kan denote sea-breeze front and Kangnung city. (b) Vertical diffusion coefficient for turbulent heat (m^2s^{-1}). CBL and TIBL denote convective boundary layer and thermal internal boundary layer. Sea (----) indicates the East Sea.

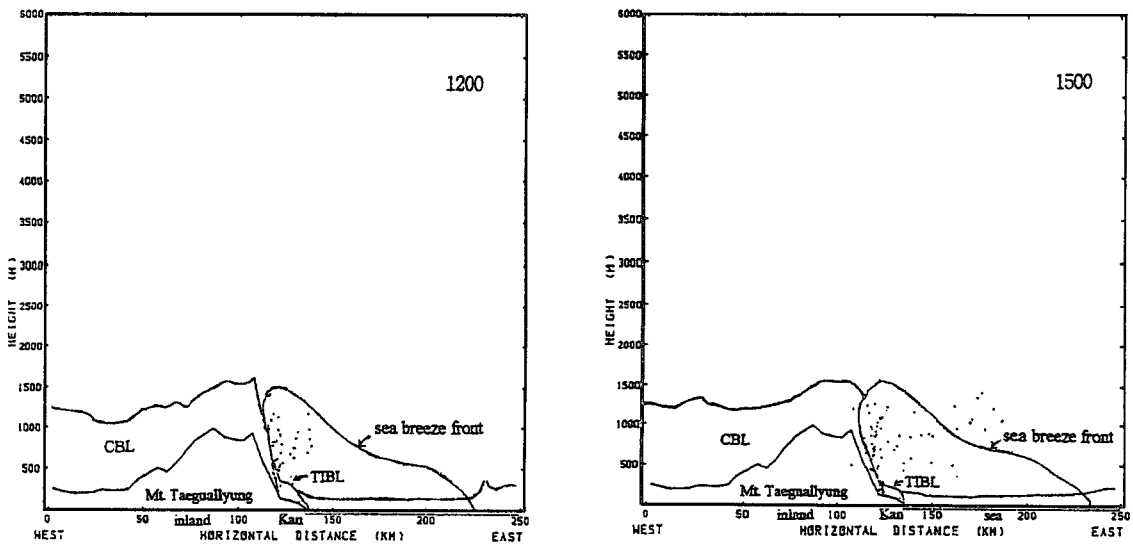

(a) (b)

Fig. 3. (a) Transportation of particulates in the coastal region near Kangnung city (Kan) under the influence of thermal internal boundary layer (TIBL) and upslope wind combined with sea-valley breeze at 1200 LST and (b) 1500 LST on August 13, 1995. CBL denotes convective boundary layer.

than at 1800 LST (Fig. 5).

Fig. 6 shows the hourly concentration of total suspended particulate (ugm^{-3}) at Kangnung city from 14 August through 15 August, 1995. At 1700 LST near sunset, the CBL with a 300 m depth due to the decrease of solar radiation became much shallower than that at 1200 LST and the TSP concentration inside the shrunken CBL became higher. Vehicle

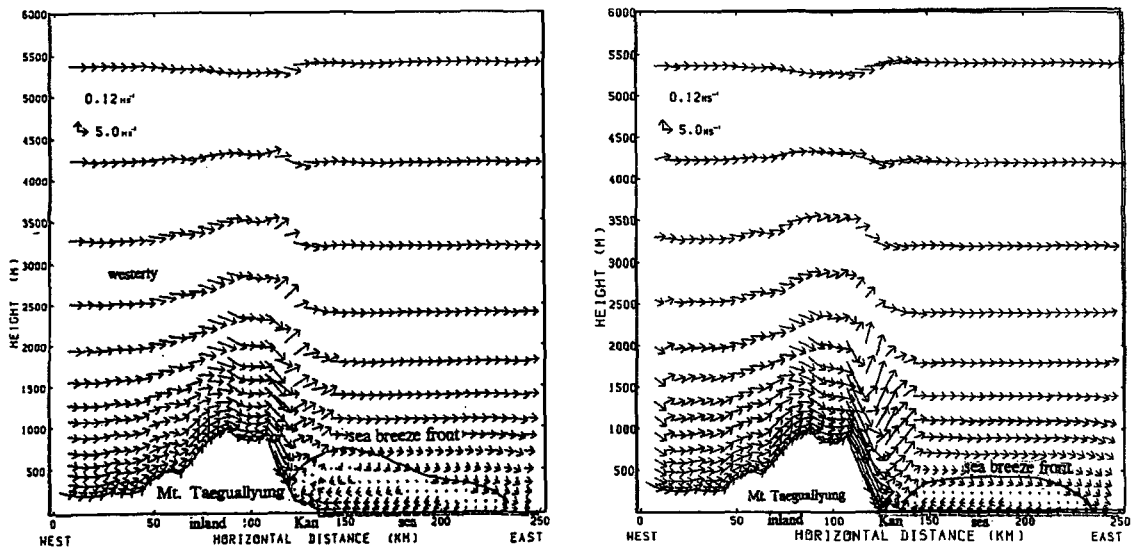

Fig. 4. (a) Vertical profiles of wind vector (ms^{-1}) on a straight cutting line (Mt. Taegeallyung-Kangnung city-East Sea) under different sea breeze circulations at 1800 LST and (b) 2100 LST, August 14, 1995.

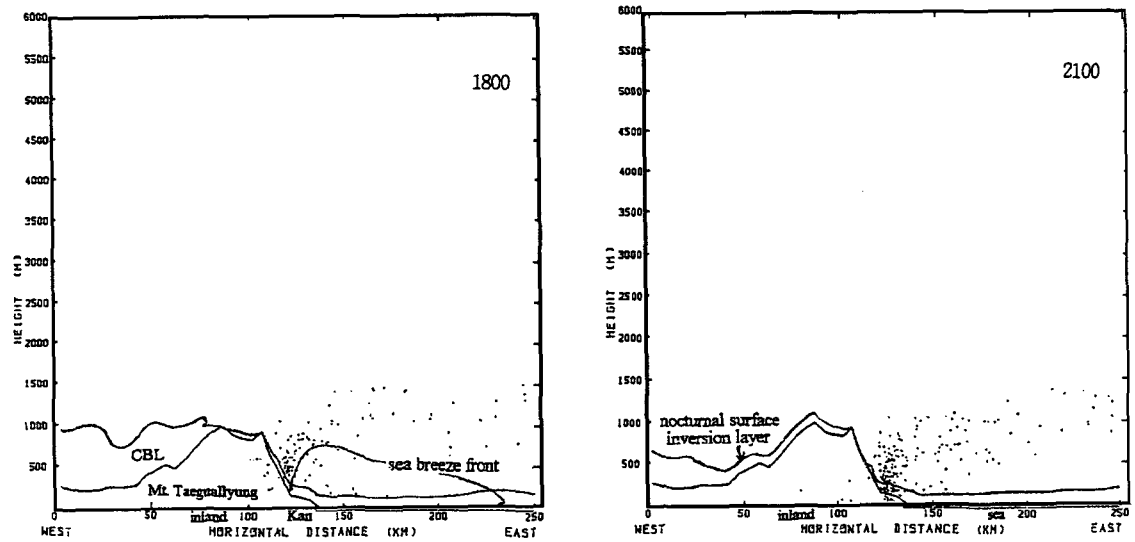

Fig. 5. (a) Transportation of particulates in the coastal region near Kangnung city (Kan) at 1800 LST and (b) 2100 LST on August 14, 1995. CBL denotes convective boundary layer.

numbers on the roads increased greatly at the end of the working day and a large amount of gases and particulates were emitted, so the TSP concentration became very high (Figs. 7 and 8). After sunset, 1800 LST, the number of vehicles gradually decreased and the emission amounts of particulates also decreased, hence lowering the TSP concentration.

As cooling of the ground surface, shortly after sunset was not big, nocturnal surface inversion layer was not much shallower than convective boundary layer near sunset. Under this condition, easterly mountain wind toward the basin was not generated and

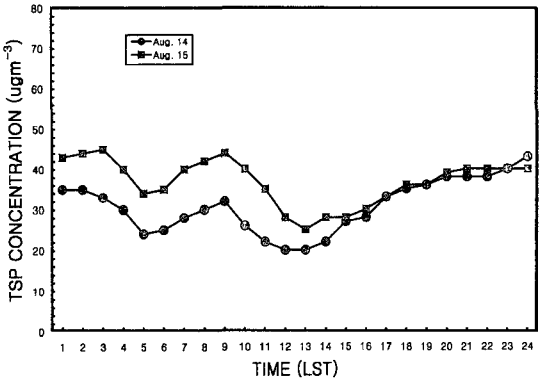

Fig. 6. Hourly concentration of total suspended particulate (ugm^{-3}) at a monitoring site of Kangnung city from August 14 through 15, 1995.

westerly wind still drove the floating particles toward the mountain until 2000 LST. The tendency of low concentration of particles in the model result well matched the measured TSP concentration by MOE[24]. After sunset, the number of released particles in the model was reduced like two particles per two minutes rather than four particles per two minutes in the daytime, due to the reduced number of vehicles on the street.

On the other hand, at 0000 LST, nighttime radiative cooling of the ground surface produces a shallow nocturnal surface inversion layer (NSIL) with a thickness of about 200 m in the basin surface, but relatively thin thickness of 100 m near the mountain surface (Figs. 7, 8 and 9). Westerly downward wind is associated with eastward land-breeze from the coast toward the sea, becoming stronger and stronger. Since the downward wind could penetrate into the city, uplifted particulate matters during the day also move down along the eastern slope of the mountain toward the downtown of the city.

Those particulates combine with the particulates released from the ground surface of the city (vehicle and house) and generated by strong surface wind, and then eastward land-breeze transports them toward the coastal sea, resulting in a maximum concentration of TSP on the ground level of the city at 0000 LST. The fallen down particulates into the coastal NSIL, in general, are dispersed toward the propagation area of internal gravity waves. At 0300 LST and 0600 LST, the particulates move into further the East Sea under the strong mountain-land breeze and some of them could be deposited on the sea surface (Figs. 10 and 11).

On the next day at 0900 LST, some of dispersed particulates over the sea surface for the nighttime hours return to the coastal inland by westward sea-breeze. Recycled particulates combine with emitted

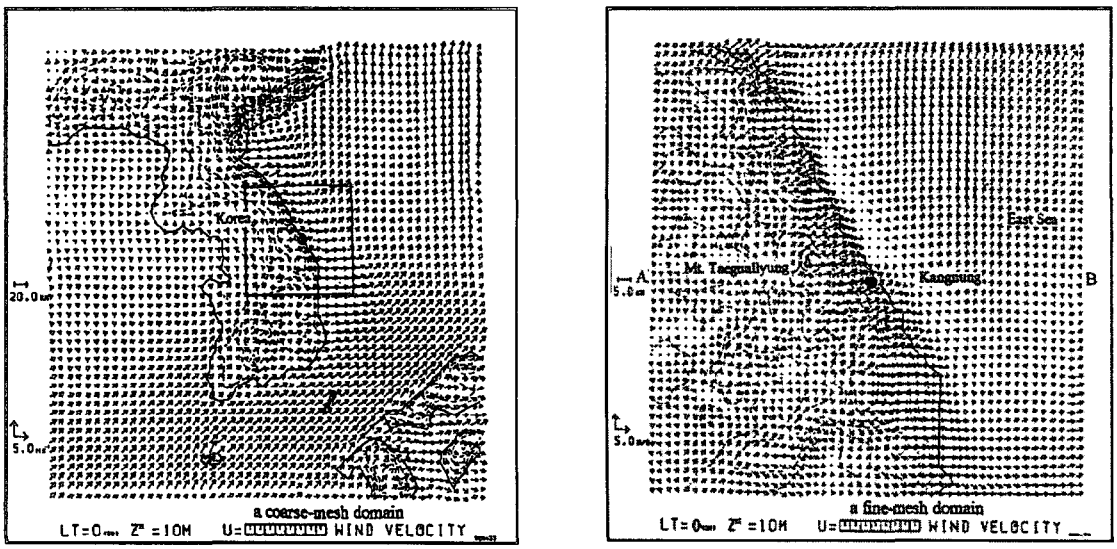

(a) (b)

Fig. 7. (a) Surface wind (ms^{-1}) in a coarse-mesh domain adjacent to Korean peninsula at 0000 LST, August 15. Thin dash line and circle o denote topography and Kangnung city. (b) A box indicates a fine-mesh domain near Kangnung city.

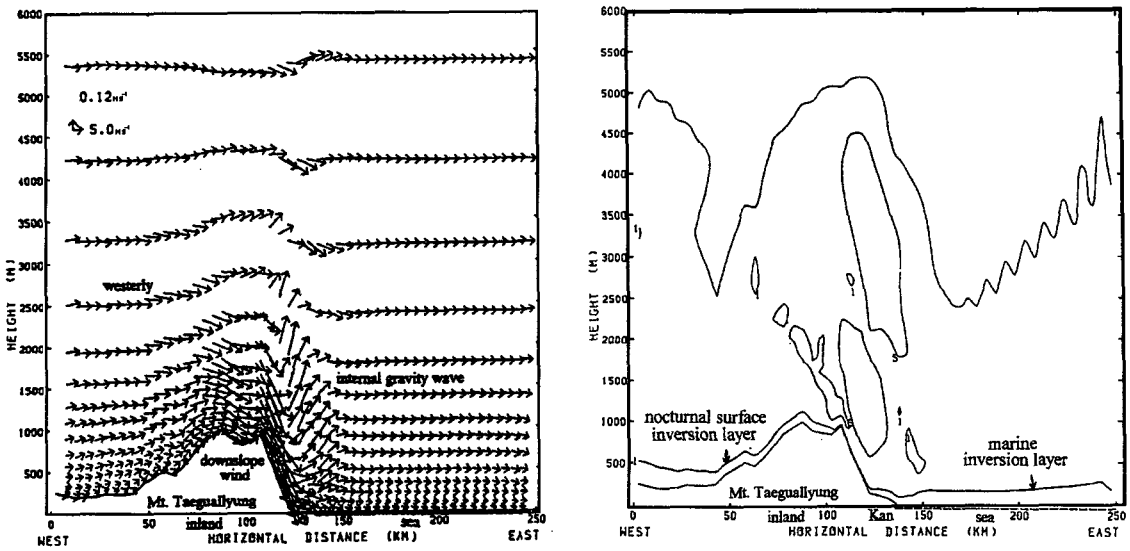

(a) (b)

Fig. 8. (a) Vertical profiles of wind vector (ms^{-1}) on a straight cutting line A-B (Mt. Taeguallyung-Kangnung city-East Sea) in a fine mesh domain of Fig. 6b at 0000 LST, August 15, 1995. (b) Vertical diffusion coefficient for turbulent heat (m^2s^{-1}).

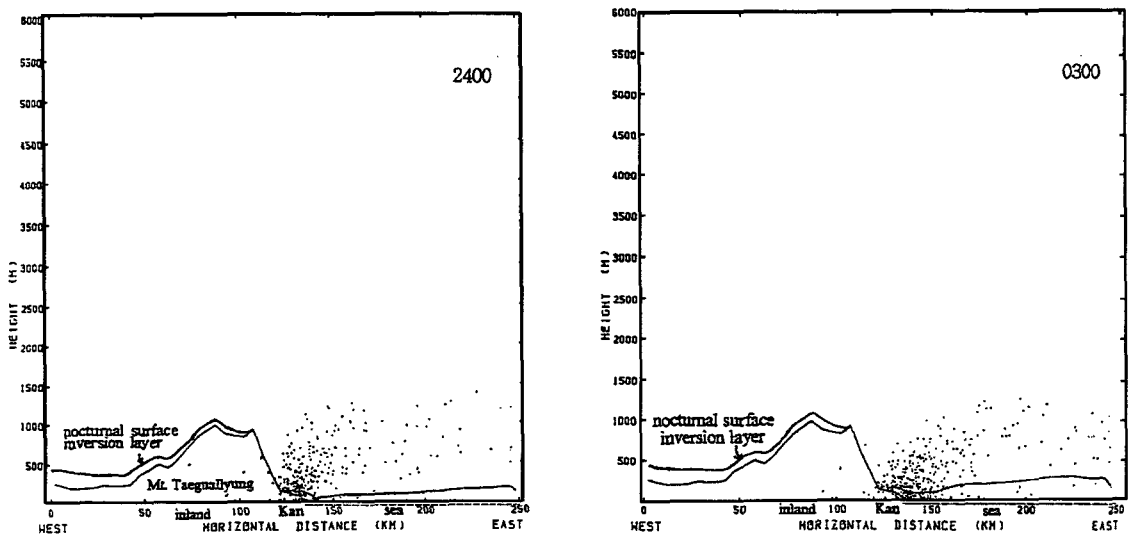

(a) (b)

Fig. 9. (a) Transportation of particulates under strong downslope wind and land breeze into Kangnung city in the coastal region (Kan) at 0000 LST and (b) maximum concentration of total suspended particulates (TSP) is found at 0300 LST on August 15, 1995. Some of them bound up toward upper level following the propagation of internal gravity waves and the others are deposited on the sea surface.

particulates from the downtown ground surface of the city in the morning and float again from the ground surface toward the top of the mountain by upslope wind (valley wind). TSP concentration at 0900 LST is relatively higher than one in the previous day. The tendency of low concentration of particles in the model result well matched the measured TSP concentration by MOE[24].

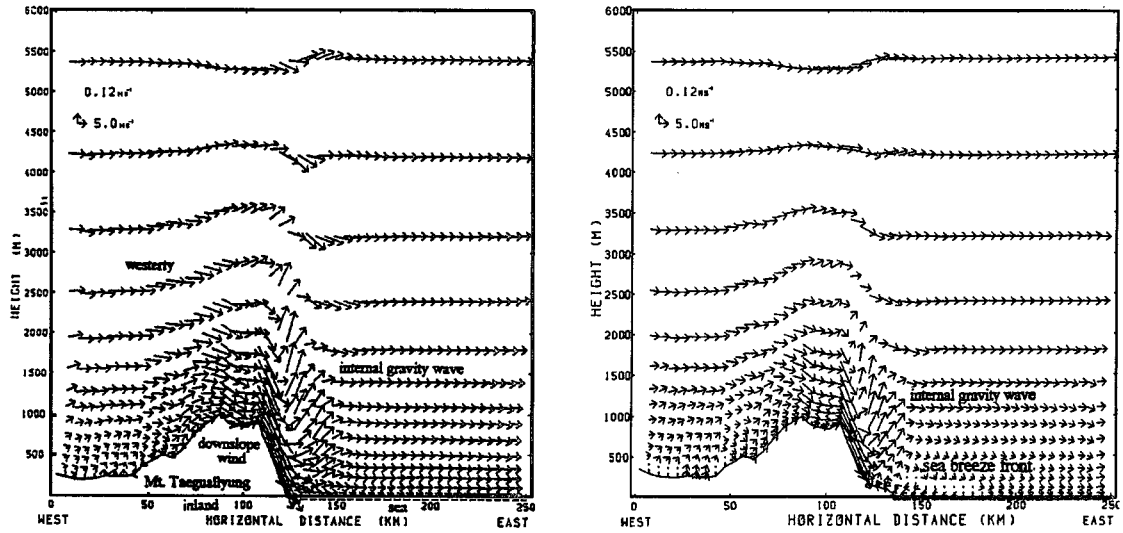

Fig. 10. (a) Vertical profiles of wind (ms^{-1}) on a straight cutting line (Mt. Taeguallyung-Kangnung city-East Sea) with maximum developments of internal gravity waves at 0600 LST, August 15, 1995. (b) Three different kinds of wind regimes such as westerly downslope wind, internal gravity and sea-breeze at 0900 LST.

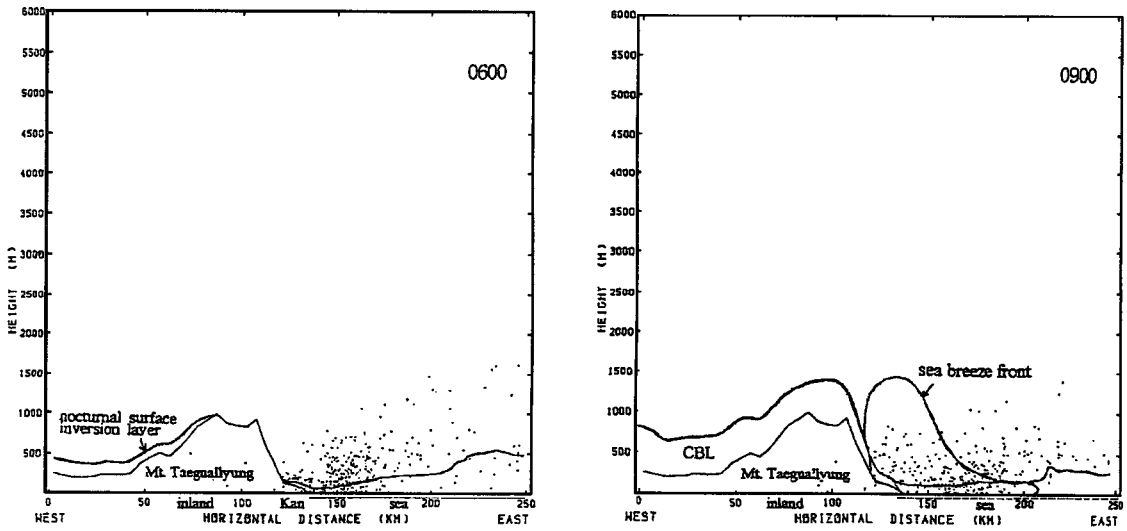

Fig. 11. (a) Transportation of particulates under strong downslope wind and land breeze into Kangnung city in the coastal region (Kan) at 0600 LST. (b) At 0900 LST, some of particulates are recycled from the sea into the city by easterly sea-breeze and combined particulates with recycled one from the sea and emitted one from the ground surface of the city in the morning float again toward the mountain top.

4. Conclusions

Convective boundary layer under synoptic scale westerly wind is developed with a thickness of about 1 km over the ground in the west of the mountain, while a thickness of TIBL is only confined to less than 200m along the eastern slope of the mountain, below an easterly sea breeze circulation. At the mid

of the eastern slop of the mountain, westerly wind confronts easterly sea breeze, which goes to the height of 1700 m above sea level and is finally eastward return flow toward the sea. Particulates floated from the ground surface of the city to the top of TIBL go along the eastern slope of the mountain in the passage of sea breeze, being away the TIBL and reach near the top of the mountain. Then those particulates disperse eastward below the height of sea-breeze circulation and widely spread out over the coastal sea. Total suspended particulate concentration near the ground surface of the city is very low.

On the other hand, nighttime radiative cooling produces a shallow nocturnal surface inversion layer with a thickness of about 200 m over the inland surface, but relatively thin thickness of less than 100m is found near the mountain surface. As synoptic scale westerly wind should be intensified under the association of mountain wind along the eastern slope of mountain to inland plain and further combine with land-breeze from inland plain toward sea, resulting in strong wind as internal gravity waves with a hydraulic jump motion bounding up to about 1km upper level in the atmosphere in the west side of the downtown of the city and becoming a eastward return flow.

Simultaneously, wind near the eastern coastal side of the city was moderate. Since the downward strong wind penetrated into the city, the particulate matters floated near the top of the mountain in the day also moved down along the eastern slope of the mountain, reaching the downtown and merging in the ground surface inside the NSIL with a maximum ground level concentration of total suspended particulates (TSP) at 0300 LST. Some of them were bounded up from the ground surface to the 1 km upper level and the others were forward to the coastal sea surface, showing their dispersions from the coastal NSIL toward the propagation area of internal gravity waves.

On the next day at 0600 LST and 0900 LST, the dispersed particulates into the coastal sea could return to the coastal inland area under the influence of sea breeze and the recycled particulates combine with emitted ones from the ground surface, resulting in relatively high TSP concentration. Later, they float again up to the thermal internal boundary layer, following sea breeze circulation.

Acknowledgements

Author would like to thank Mr. Takahashi at Japan Meteorological Agency for his useful and critical comments. This study was partially supported by a grant-in-aid for scientific research project of Dual use technology-virtual marine environmental analysis technology for operation from Ministry of Science and Technology in 1999-2001.

References

1) Choi, H., 2003, Increase of ozone concentration in an inland basin during the period of nocturnal thermal high, Water, Air and Soil Poll. Focuss, 3, 31-51.
2) Diehl, S., D. Smith and M. Sydor, 1982, Radom walk simulation of gradient-transfer processes applied to dispersion of stack emission from coal-fired power plant, J. Applied. Meteor., 69, 69-83.
3) Kimura, F. and S. Takahashi, 1991, The effects of land-use and anthropogenic heating on the surface temperature in the Tokyo metropolitan area: numerical experiment, Atmos. Environ., 25, 155-164.
4) Kuwagata, T. and M. Sumioka, 1991, The daytime PBL heating process over complex terrain in central Japan under fair and calm weather conditions. Part III: Daytime thermal low and nocturnal thermal high, J. Meteor. Soc. Japan, 69, 91-104.
5) Ross, D. G, A. M. Lewis and G. D. Koutsenko, 1999, Comalco (bell bay) local airborne contaminant transport study: Airshed modeling system, development and evaluation, Proceed. of fifth joint seminar on regional deposition process in the atmosphere, Seoul, 43-52pp.
6) Baird, C., 1995, Environmental Chemistry, New York: W. H. Freeman and Company, 484pp.
7) Moller, D., 2001, Photo-oxidation capacity, Proceed. of workshop on local and regional contribution to air pollution and local radiative balance in Asian developing countries, Guangzhou, China, 16-16.
8) Park, S. U. and J. Y. Moon, 2001, Lagrangian particle dispersion modeling in the complex coastal terrain of Korea, J. Korean Meteor. Soc., 37, 225-238.

9) Xuan, J., 1999, Vertical fluxes of dust in northern Asia. Proceed. of fifth joint seminar on regional deposition process in the atmosphere, Seoul, 43-52pp.
10) PU, 1995, The effects of particles and gases on acid depositions and parameterization, Technical Report of State Key Project, 85-912-01-04-05, 250pp.
11) JMRI, 1995, Manual of random walk model revised by Japan Meteorological Research Institute, 10pp.
12) NFRADA, 1998, Analyzed NOAA satellite pictures on the sea surface temperature, National Fisheries Research and Development Agency.
13) Kimura, F. and S. Arakawa, 1983, A numerical experiment of the nocturnal low level jet over the Kanto plain, J. Meteor. Soc. Japan, 61, 848-861.
14) Takahashi, S., 1998, Manual of LAS model revised by Dr. Sato, Meteorological Research Institute, Japan Meteorological Agency, 50pp.
15) Klemp, J. B. and D. R. Durran, 1983, An upper condition permitting internal gravity wave radiation in numerical meso-scale model, Mon. Wea. Rev., 111, 430-440.
16) Orlanski, I., 1976, A simple boundary condition for unbounded hyperbolic flows, J. Comp. Phys., 21, 251-269.
17) Yamada, T., 1983, Simulation of nocturnal drain age flows by a q2-l turbulence closure model, J. Atmos Sci., 40, 91-106.
18) Yamada, T. and G. L. Mellor, 1983, A numerical simulation of the BOMEX data using a turbulence closure model coupled with ensemble cloud relations, Q. J. R. Meteor. Soc., 105, 95-944.
19) Katayama, A., 1972, A simplified scheme for computing radiative transfer in the troposphere, Technical report. 6, Dept. of Meteor., U.C.L.A., 77pp.
20) Businger, J. A., 1973, Turbulence transfer in the atmospheric surface layer, Proceed. of workshop on Micrometeorology (D. A. Haugen, ed), Amer. Meteor. Soc., 54, 67-100.
21) Monin, A. S., 1970, The atmospheric boundary layer, Annual Rev. Fluid Mech., 2, 225-250.
22) Deardoff, J. W., 1978, Efficient prediction of ground surface temperature and moisture with inclusion of a layer of vegetation, Geophys Res., 38, 659-661.
23) Kimura, F. and T. Yoshikawa, 1988, Numerical simulation of global scale dispersion of radioactive pollutants from the accident at the Chernobyl Nuclear Power Plant, J. Meteor. Soc. Japan, 66, 489-495.
24) MOE, 1995, Hourly measured data of atmospheric pollutants. Ministry of Environment, Korea, 150pp.